Desalination and Water Treatment
www.deswater.com
doi: 10.5004/dwt.2023.29217

283 (2023) 247–258
January

Application of United Arab Emirates *Arecaceae* leaves biochar for adsorptive removal of Rhodamine B from an aqueous solution

Muhammad Imran Khan[a,*], Abdallah Shanableh[a], Suryyia Manzoor[b], Aziz ur Rehman[c], Shabnam Shahida[d], Fawad Ahmad[e]

[a]*Research Institute of Sciences and Engineering (RISE), University of Sharjah, Sharjah 27272, United Arab Emirates, emails: raoimranishaq@gmail.com/mimran@sharjah.ac.ae (M.I. Khan), shanableh@sharjah.ac.ae (A. Shanableh)*
[b]*Institute of Chemical Sciences, Bahauddin Zakariya University, Multan 60800, Pakistan, email: suryyia.manzoor@bzu.edu.pk*
[c]*Institute of Chemistry, The Islamia University of Bahawalpur, Bahawalpur 63100, Pakistan, email: azizypk@yahoo.com*
[d]*Department of Chemistry, University of Poonch, Rawalakot 12350, Azad Kashmir, Pakistan, email: shabnamshahida01@gmail.com*
[e]*Department of Chemistry, University of Wah, Wah Cantt 47040, Pakistan, email: fawad.ahmad@uow.edu.pk*

Received 16 July 2022; Accepted 9 December 2022

ABSTRACT

This article reports the application of United Arab Emirates (UAE) *Arecaceae* leaves biochars for adsorptive removal of Rhodamine B (RhB) from an aqueous solution at room temperature. Adsorption of RhB onto *Arecaceae* leaves biochar was proved by using Fourier-transform infrared spectroscopy. The morphology of *Arecaceae* leaves biochar was investigated by scanning electron microscopy. The influence of operational parameters on the percentage removal of RhB was explored in detail. Results showed that the percentage removal of RhB was increased with contact time and mass of UAE *Arecaceae* leaves biochar, whereas presented an inverse relation with initial concentration of RhB dye solution as well as temperature. Adsorption kinetics study showed that RhB adsorption onto UAE *Arecaceae* leaves biochar fitted to pseudo-second-order kinetics rendering the value of correlation coefficient (R^2 = 0.998) close to unity. Several adsorption isotherms were used to explore adsorption of RhB onto UAE *Arecaceae* leaves biochars. Results represented that RhB adsorption onto *Arecaceae* leaves biochars fitted well to Langmuir isotherm with correlation coefficient value close to unity (R^2 = 0.999). The values of Gibb's free energy ($\Delta G°$), enthalpy ($\Delta H°$), and entropy ($\Delta S°$) were measured to study adsorption thermodynamics for the dye onto *Arecaceae* leaves biochars. Attained results represented that RhB adsorption from an aqueous solution onto *Arecaceae* leaves biochars was an exothermic process ($\Delta H°$ = –16.30 kJ/mol). The positive value of Gibb's free energy showed that RhB adsorption was a non-spontaneous process.

Keywords: UAE *Arecaceae* leaves biochar; Rhodamine B; Non-spontaneous process; Pseudo-second-order model; Physical adsorption process

1. Introduction

Water pollution is one of the most serious environmental issues being faced by the living organisms, among which, dyes have contributed enormous damage to water bodies and also greatly impact human health due to their high toxicity and carcinogenicity [1]. Rhodamine B (RhB) is a synthetic carcinogenic cationic xanthene dye, widely used in textile printing and dyeing, leather, colored glass, paint and other industries can also be used as biological dyeing and organic reagent for some metals detection [2]. RhB wastewater with high chromaticity discharged into the water, not only disturbs the landscape, but also reduces the transmittance of light and hinders the photosynthesis

* Corresponding author.

of aquatic plants [3]. In the degradation process, RhB may be converted into more toxic intermediate products, which could accumulate in the environment and organisms for a long term, ultimately causing serious impact and harms to the natural environment, animals and plants [4,5]. Therefore, it is imperative to find an efficient and simple method to remove RhB.

A variety of methods such as electrooxidation, advanced oxidation processes (AOPs), coagulation and flocculation, adsorption, biological degradation and membranes processes were utilized for decoloration and degradation of dyestuff from wastewater [6,7]. Among these methods, adsorption is most extraordinary one for dye removal from an aqueous solution due to its simplicity, high efficiency, and ease of operation as well as the presence of a wide range of adsorbents [8,9]. Besides, it is favorable method because of low cost, regeneration of adsorbent, applicability for wide range of adsorbate, no pre-treatment needs, and non-extended of harmful residues [7,10,11].

Several adsorbents which exhibited excellent capability were already investigated [12,13]. The commercially activated carbon is highly efficient for the removal of color but its high cost has blocked its large-scale application [14]. Many adsorbents such as hen feather [15], layered double hydroxides (LDHs) [16], walnut husk [17], synthesized metal- and halide-free variant of ordered mesoporous carbon (OMC) [10], metal–organic framework (MOF) [18], chitosan grafted polyaniline-OMMT nanocomposite [19], OMC [20], biomass of penicillium YWO1 [21], Kahwa tea (*Camellia sinensis*) carbon [22], ash of black turmeric rhizome [23], biochars from crop residues [24], papaya peel carbon [25], *Curcuma caesia* based activated carbon [26], Ag doped MnO_2-CNT nano-composite [27], OMC [28], guar gum/activated carbon nanocomposite [29], polymeric ion exchange membranes [8,30,31], composites [32], natural zeolite [33], natural clinoptilolite [34], sesame hull [35], etc. were applied as adsorbents for the discharge of dyes from an aqueous solution. Agriculture by-products represented its efficiency as a low-cost adsorbent and they mostly required chemical treatment to enhance adsorption performance toward dyes [36]. Contrary, some adsorbents did not exhibit higher adsorption efficiency for the anionic dyes due to their anionic or hydrophobic surfaces [14]. Therefore, it is of utmost importance to find most efficient and low-cost adsorbent for the removal of dyes from an aqueous solution.

In this research, the application of United Arab Emirates (UAE) *Arecaceae* leave biochars for the adsorption of RhB from an aqueous solution was explored at room temperature. The adsorptive removal of RhB by using UAE *Arecaceae* leaves biochars has not been reported yet to the best of our knowledge. Fourier-transform infrared spectroscopy (FTIR) was employed to confirm adsorption of RhB onto *Arecaceae* leaves biochar. The morphology of *Arecaceae* leaves biochar was evaluated by scanning electron microscopy in detail. The inluence of operating parameters including contact time, mass of *Arecaceae* leaves biochar, initial concentration of RhB in aqueous solution and temperature on the percentage removal of RhB was revealed in detail. For RhB adsorption onto *Arecaceae* leaves biochar, adsorption isotherm, kinetic and thermodynamic investigations were also conducted.

2. Experimental

2.1. Materials

Rhodamine B (RhB), sodium hydroxide (NaOH) and hydrochloric acid (HCl) were purchased from Sinopharm Chemical Reagent Co., Ltd., China. The *Arecaceae* leaves were obtained from local *Arecaceae* trees present in the sustainability garden of the University of Sharjah, Sharjah, United Arab Emirates (UAE). All the chemicals were utilized as received. Deionized (DI) water was utilized throughout the work.

2.2. Preparation of palm leaves biochar (adsorbent)

Initially, the *Arecaceae* tree leaves (biomass) were cleaned with deionized (DI) water repeatedly to withdraw dust particles. After that, they were cut into 1–2 cm length pieces and oven dried at 80°C for 12 h to evaporate water and moisture content. The ultra-centrifugal mill (Model ZM 200, Retsch, Germany) at (< 0.25 mm) mesh was used to grind the dried palm leaves (biomass). It was then converted to biochar by pyrolysis for 60 min at 550°C employing a heating rate of 10°C/min. The flow of nitrogen gas (200 mL/min) using quartz tube furnace (Model STG-110-17, SAF Therm, China) was used to conduct pyrolysis process. The process of preparation *Arecaceae* leaves biochar is shown in Fig. 1.

2.3. Adsorbate

In this research, Rhodamine B (RhB) was employed as a model pollutant. The molecular formula is $C_{28}H_{31}ClN_2O_3$. Its molar mass is 479.02 and structure is represented in Fig. S1.

2.4. Batch adsorption of RhB

Batch RhB adsorption from an aqueous solution onto UAE *Arecaceae* leaves biochar was performed as reported in our previous work (Section S1 for detail in Supporting information) [14,30,37–39].

2.5. Instrumentations

The biochar before and after RhB adsorption was studied by using FTIR spectrometer (Vector 22, Bruker, Massachusetts, MA, USA) containing resolution of 2 cm^{-1} and total spectral range of 4,000–400 cm^{-1} by utilizing attenuated total reflectance (ATR). Morphology was studied by using field-emission scanning electron microscope (FE-SEM, SIRION 200, FEI Company, USA).

2.6. Adsorption isotherms

Experimental data for RhB adsorption onto biochar was subjected to several adsorption isotherms including Langmuir, Freundlich, Temkin and Dubinin–Radushkevich (D-R) (Section S2 for detail in Supporting information).

2.7. Adsorption kinetics

Adsorption kinetics for RhB adsorption was illustrated by using kinetic models such as pseudo-first-order,

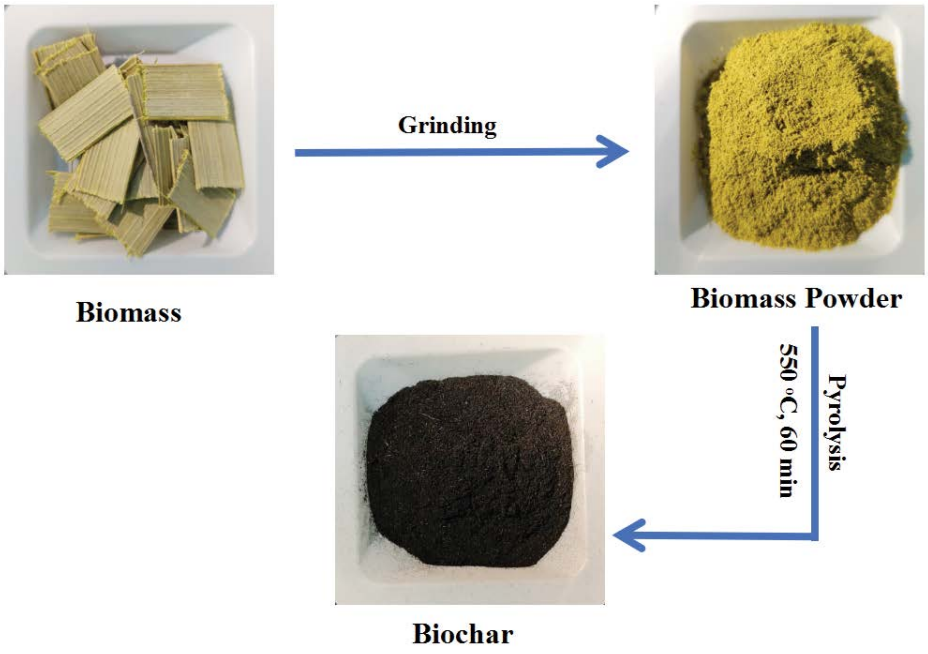

Fig. 1. Preparation of *Arecaceae* leaves biochars.

pseudo-second-order, Elovich model, liquid-film diffusion model, modified Freundlich equation and Bangham equation (Section S3 for detail in Supporting information).

2.8. Adsorption thermodynamics

The change in Gibb's free energy ($\Delta G°$), enthalpy ($\Delta H°$) and entropy ($\Delta S°$) were measured to study adsorption thermodynamics as described (Section S4 for detail in Supporting information) [7,14].

3. Results and discussion

3.1. Fourier-transform infrared spectroscopy

The successful RhB adsorption onto *Arecaceae* leaves biochar was proved by using FTIR spectroscopy and attained results are shown in Fig. S2. The broad peak at 3,339 cm^{-1} was associated to the O–H stretching vibration of carboxylic acid alcohol and phenol groups of *Arecaceae* leaves [40]. The peak around 1,630 cm^{-1} was ascribed to C=C bond in aromatic ring and it can also represent H–O–H bending band of water [41,42]. The peak in between 484 cm^{-1} was related to aromatic C–H groups of *Arecaceae* leaves [40]. The peak at 2,941 and 2,847 cm^{-1} were attributed to alkyl (–CH) and C=O stretching vibration [43] and also the peak at 1,738 cm^{-1} was due to C–O of carboxyl, aldehyde, ketone, and ester groups. The peak at 1,444 cm^{-1} was attributed to aliphatic C–H, the peak located at 1,114 cm^{-1} was assigned to C–O–C in cellulose and hemicelluloses.

After RhB adsorption onto *Arecaceae* leaves biochar, the peak intensities decreased significantly which proved RhB's adsorption onto palm leaves biochar from an aqueous solution.

3.2. Morphology

Adsorption of dyes is dependent on morphology of adsorbents. Morphology of *Arecaceae* leaves biochar was revealed by using scanning electron microscopy (SEM). Attained micrograph is shown in Fig. S3. It was observed that morphology of *Arecaceae* leaves biochar was uneven. The rough surface can enhance the adsorption of dye by increasing the surface area of the adsorbent. The surface of *Arecaceae* leaves biochar showed pores on it. This porous structure of biochar can further result in an increase of RhB adsorption from an aqueous solution.

3.3. Effect of operating factors

3.3.1. Effect of contact time

The removal of RhB from an aqueous solution was highly dependent on contact time. The effect of contact time on the removal of RhB was demonstrated by varying time from 30 to 1,440 min. Fig. 2a represents the influence of contact time on the percentage removal of RhB from an aqueous solution at room temperature. The removal of RhB was enhanced with enhancing contact time. Fig. 3 gives an interesting comparison of RhB removal performance of biochar with other reported adsorbents reported in literature. Results showed that the percentage removal of RhB was increased from 54% to 94% with increase in contact time. As represented in Fig. 2a, the removal of RhB was rapid in the beginning because of presence of several empty sites for RhB adsorption onto the biochar surface. The removal of RhB was slowed with time passage. It achieved saturation after 300 min. It denoted that equilibrium was occurred after 300 min. This optimum time was employed for conduction of future experiments.

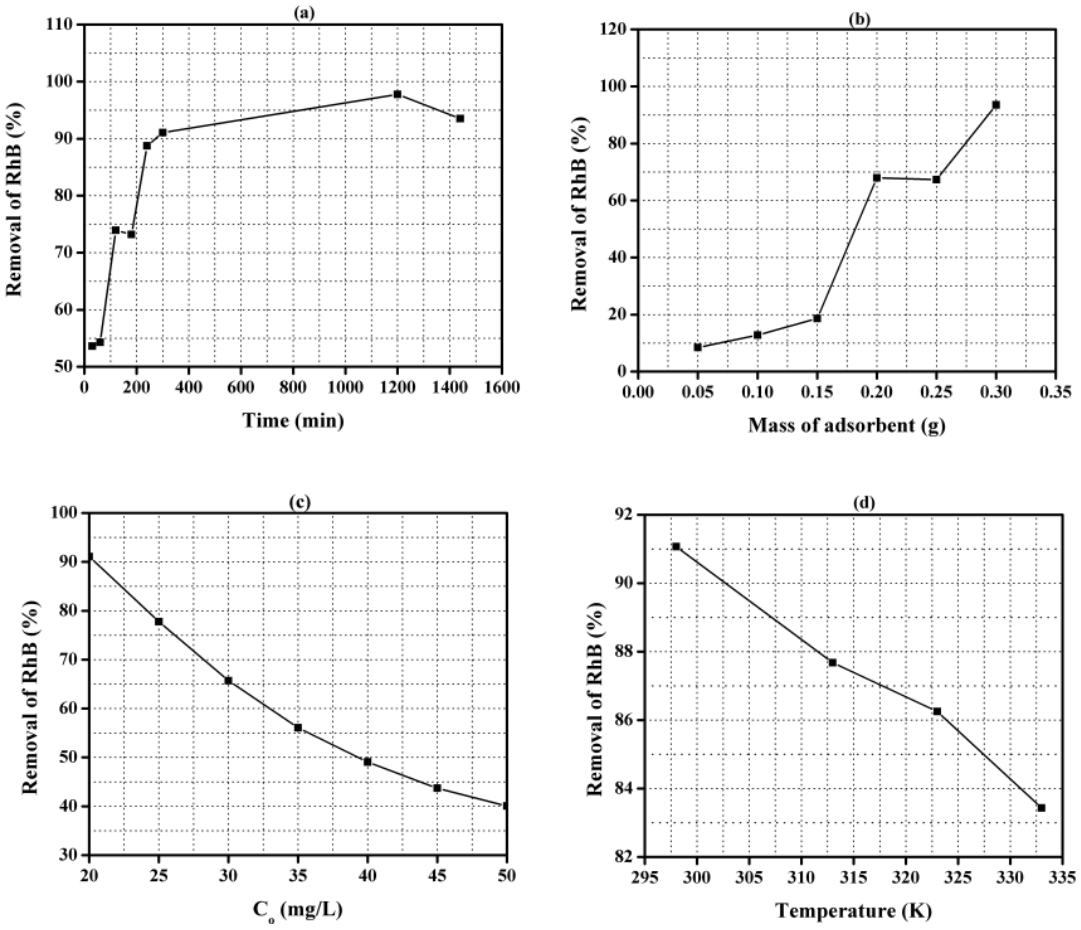

Fig. 2. (a) Effect of contact time (initial concentration of RhB = 20 mg/L, amount of biochars = 0.30 g), (b) effect of mass of biochar (initial concentration of RhB = 20 mg/L, contact time = 1,440 min), (c) effect of initial concentration of RhB dye solution (contact time = 1,440 min, amount of biochars = 0.30 g), and (d) effect of temperature onto the removal of RhB from aqueous solution by biochar (initial concentration of RhB = 20 mg/L, contact time = 1,440 min, amount of biochars = 0.30 g).

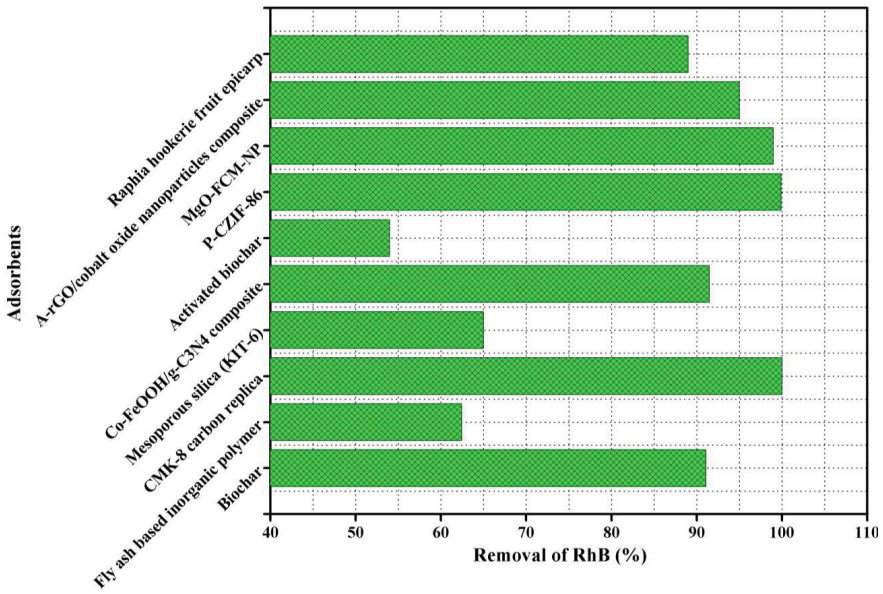

Fig. 3. Comparison of RhB removal performance of biochar with other reported adsorbents [44–51].

3.3.2. Effect of mass of biochars

The effect of mass of biochars on RhB removal at room temperature was investigated by changing mass of biochars from 0.05 to 0.30 g. Fig. 2b shows the effect of masses of biochar on the percentage removal of RhB. It was observed that the removal of RhB was enhanced from 8% to 94% with increasing the mass of biochars. It was associated to increase in number of active sites with enhancing mass of biochars from 0.05 to 0.30 g. Similar results were reported in our previous work [7,8,14].

3.3.3. Effect of initial concentration

Fig. 2c depicts the effect of initial concentration on the percentage removal of RhB from an aqueous solution at room temperature. Attained results exhibited a decrease in percentage removal of RhB from 91% to 40% with increase in initial concentration of RhB in an aqueous solution. The decrease in percentage removal was associated to saturation of the active sites of the biochar by increasing the initial concentration of RhB into an aqueous solution [14,30].

3.3.4. Effect of temperature

The effect of temperature on the percentage removal of RhB from an aqueous solution by using biochars was studied and attained results are presented in Fig. 2d. A decline in percentage removal of RhB was observed with rise in temperature. It was found that the removal of RhB decreased from 91% to 83% with increase in temperature from 298 to 333 K. It showed that adsorption of RhB from an aqueous solution onto biochars was an exothermic process.

3.4. Adsorption kinetics for RhB adsorption onto biochar

Adsorption kinetics were evaluated by employing several adsorption kinetic models such as pseudo-first-order, pseudo-second-order, Elovich model, liquid-film diffusion model, modified Freundlich equation and Bangham equation. Fig. 4a depicts the plot of pseudo-first-order model for RhB adsorption onto biochar. The correlation coefficient (R^2) value was 0.912. The adsorption capacity (q_e) was determined from intercept of the plot of pseudo-first-order model and is given in Table 1. There was a large difference between the values of experimental adsorption capacity (1.25 mg/g) and calculated adsorption capacity (4.40 mg/g). Hence, pseudo-first-order model can't explain the rate process for RhB adsorption onto biochar. The graphical representation of pseudo-second-order model is shown in Fig. 4b. The determined adsorption capacity value (1.30 mg/g) is given in Table 1 which was in good agreement with the experimental adsorption capacity (1.25 mg/g). The correlation coefficient value (R^2 = 0.998) for pseudo-second-order model was close to unity. Therefore, RhB adsorption onto biochar fitted well to pseudo-second-order model. Fig. 4c denotes the plot of Elovich model and the calculated values of its factors (α and β) are given in Table 1. The correlation coefficient value (R^2 = 0.828) was smaller than pseudo-second-order model. Therefore, it was not convenient to explain RhB adsoprtion onto biochar

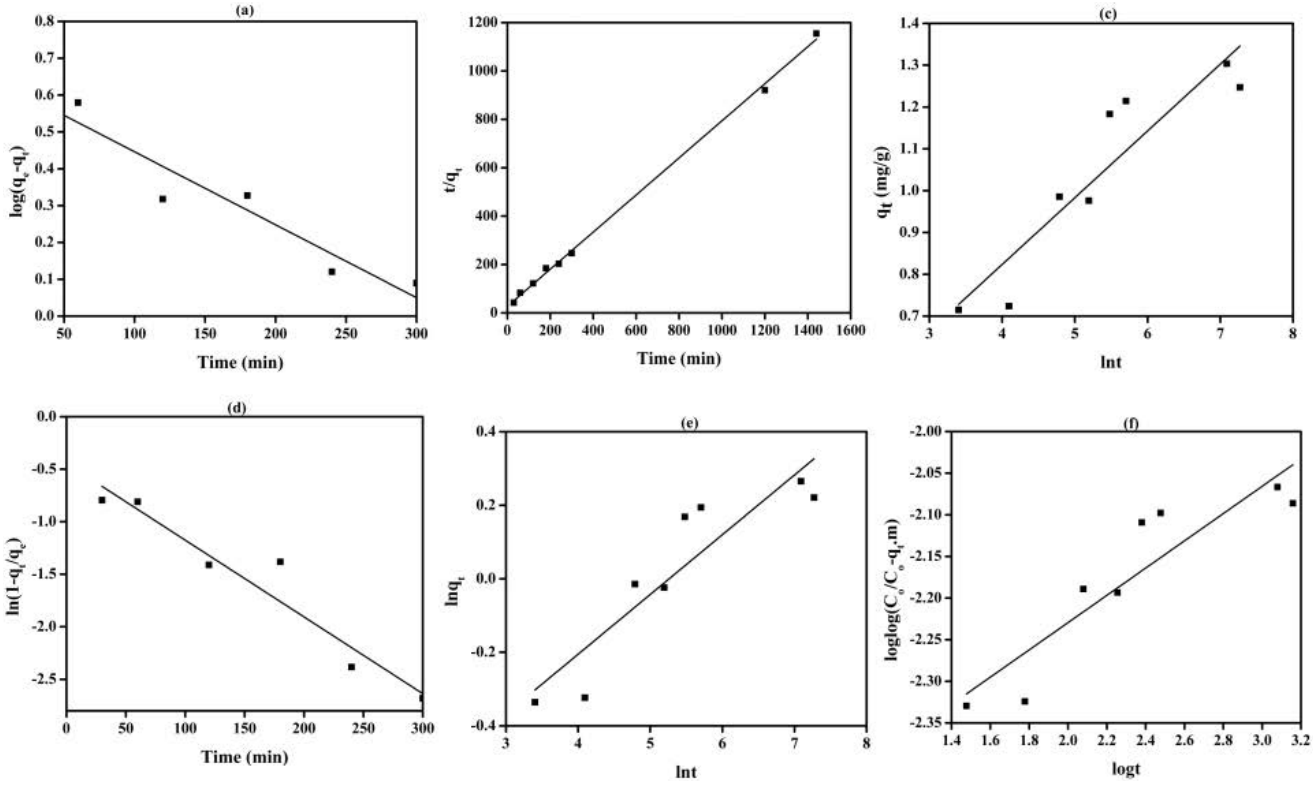

Fig. 4. (a) Pseudo-first-order model, (b) pseudo-second-order model, (c) Elovich model, (d) liquid-film diffusion model, (e) modified Freundlich equation and (f) Bangham equation for RhB from an aqueous solution onto biochar.

Table 1
Calculated values of kinetic parameters for adsorption of RhB onto United Arab Emirates *Arecaceae* leaves biochar

Kinetic models	Measured parameters	
Pseudo-first-order model	$q_{e,\text{exp.}}$	1.25
	$q_{e,\text{cal.}}$	4.40
	$k_1 \times 10^{-3}$	1.98
	R^2	0.912
Pseudo-second-order model	q_e	1.30
	$k_2 \times 10^{-2}$	2.16
	R^2	0.998
Elovich model	α	0.52
	β	6.25
	R^2	0.828
Liquid-film diffusion model	$K_{\text{fd}} \times 10^{-3}$	7.31
	C_{fd}	–0.44
	R^2	0.916
Modified Freundlich equation	m	6.15
	$K \times 10^{-2}$	2.10
	R^2	0.802
Bangham equation	k_o	0.42
	α	0.16
	R^2	0.802

q_e: mg/g; k_1: (min^{-1}); k_2: g/mg·min; α: mg/g·min; β: g/mg; K_{fd}: (min^{-1}); K: L/g·min; k_o: mL/g·L

Table 2
Measured parameters of adsorption isotherm for adsorption of RhB onto United Arab Emirates *Arecaceae* leaves biochar

Adsorption isotherms	Measured parameters	
Langmuir isotherm	Q_m	1.33
	K_L	4.76
	R^2	0.999
Freundlich isotherm	R_L	0.0042–0.010
	n	35.71
	k_F	1.21
	R^2	0.785
Temkin isotherm	A_T	1.03×10^{15}
	b_T	69,954
	R^2	0.788
D-R isotherm	q_e	1.31
	β	0.067
	R^2	0.936
	E	2.70

Q_m (mg/g); K_L (L/mol); k_F ((mg/g)(L/mg)$^{1/n}$); C_m (mol/g); β (mol^2/J^2); E (kJ/mol)

from an aqueous solution. The grphical respresentation of liquid-film diffusion model is shown in Fig. 4d and the measured value of K_{fd} is given in Table 1. The correlation coefficient value (R^2 = 0.916) was smaller than pseudo-second-order model. Hence, it can't explain RhB adsorption onto biochar from an aqueous solution. The plot of modified Freundlich equation for RhB adsorption is represented in Fig. 4e. The determined values of its factors are given in Table 1. The correlation coefficient value (R^2 = 0.802) was quite less than 1 suggesting its unsuitability for RhB adsorption onto biochar from an aqueous solution. In addition, the Bangham equation plot is represented in Fig. 4f and the determined values of its factors are given in Table 1. The double logarithmic plot did not give linear curves showing that the diffusion of adsorbate (RhB) into pores of the adsorbent (biochar) is not the only rate controling step [31,52]. It may be that both film and pore diffusion were crucial to different extent for adsorpion of RhB onto biochar from wastewater.

3.5. Adsorption isotherms

Experimental data for RhB adsorption onto biochars was subjected to several adsorption isotherms such as Langmuir isotherm, Freundlich isotherm, Temkin isotherm and Dubinin–Radushkevich (D-R) isotherm. Fig. 5a represents Langmuir adsorption isotherm for RhB adsorption from an aqueous solution onto biochars and the attained values of its factors are shown in Table 2. The correlation coefficient (R^2 = 0.999) value was close to unity representing that RhB adsorption onto biochar fitted to Langmuir isotherm. The R_L value (0.0042–0.010) represented that RhB adsorption was a favorable process. Fig. 5b depicted Freundlich adsorption isotherm for RhB adsorption and the obtained values of its factors are represented in Table 2. The correlation coefficient value (R^2 = 0.785) showed that RhB adsorption followed Freundlich adsorption isotherm. The value of Freundlich constant 'n' was found to be 1.21 suggesting that RhB adsorption onto biochar was favorable because the value of "n" ranges from 2–10 representing good adsorption, 1–2 moderate adsorption and less than one shows poor adsorption [7,14]. Temkin isotherm for RhB adsorption onto biochars is shown in Fig. 4c. Attained values of b_T and A_T are given Table 2. The correlation coefficient value (R^2 = 0.788) denoted that RhB adsorption onto biochars followed Temkin isotherm. Fig. 4d denotes D-R adsorption isotherm for RhB adsorption onto biochar. The determined values of its endowments are given in Table 2. Attained value of mean adsorption energy (E) was 2.70 kJ/mol. It showed that RhB adsorption onto biochar was physical adsorption process [53,54]. The value of E higher than 8 kJ/mol means chemical ion exchange adsorption process whereas the value of E lower than 8 kJ/mol is the characteristic of physical adsorption process [55].

3.6. Adsorption thermodynamics

The changes in Gibb's free energy (ΔG°), enthalpy (ΔH°), and entropy (ΔS°) were measured to explore adsorption thermodynamics for RhB adsorption onto biochar. Fig. 6 represents the plot of $1/T$ vs. $\ln K_c$ for RhB adsorption onto *Arecaceae* leaves biochar. The determined values of thermodynamic factors are represented in Table 3. As shown in Table 3, the value of enthalpy (ΔH° = –16.30 kJ/mol) was negative respresenting that RhB adsorption onto biochar was exothermic process whereas the negative value of entropy

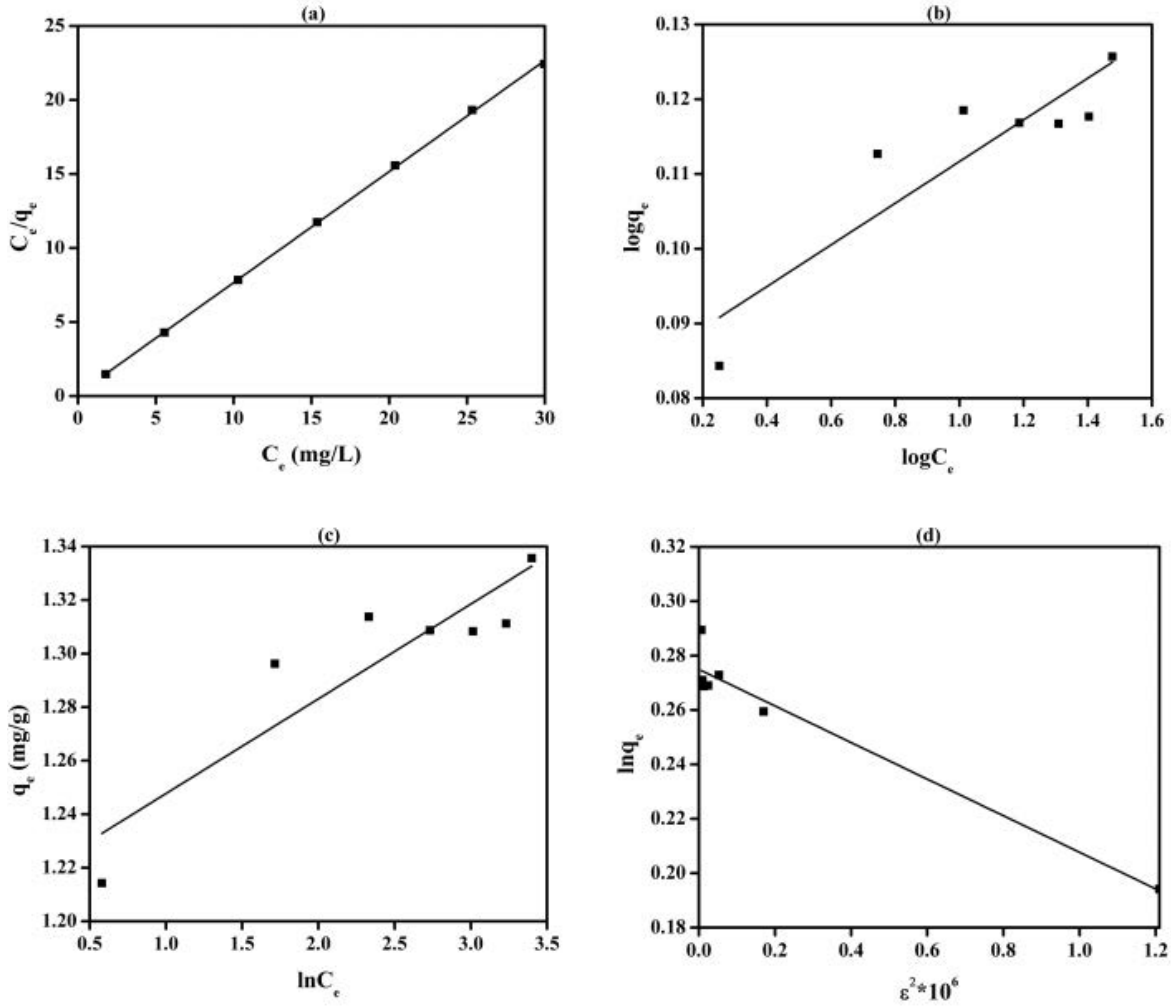

Fig. 5. (a) Langmuir isotherm, (b) Freundlich isotherm, (c) Temkin isotherm and (d) Dubinin–Radushkevich (D-R) isotherm for RhB adsorption of RhB from an aqueous solution onto biochar.

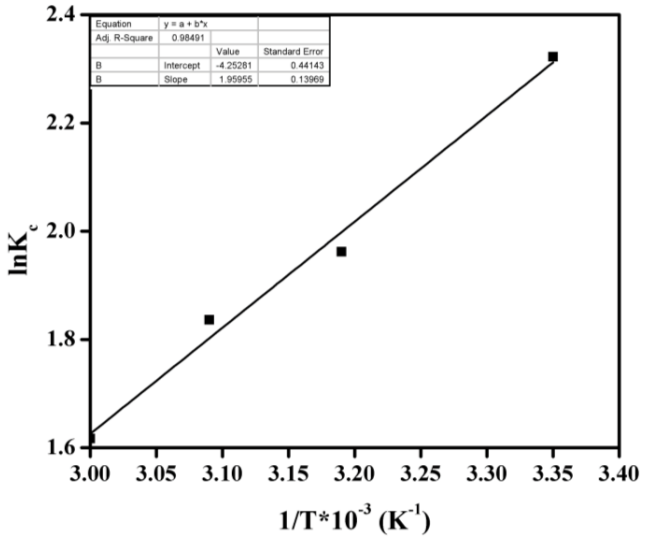

Fig. 6. Plot of 1/*T* vs. lnK_c for RhB adsorption onto *Arecaceae* leaves biochars.

Table 3
Determined thermodynamic parameters for RhB adsorption onto United Arab Emirates *Arecaceae* leaves biochar

Temperature (K)	Δ*H* (kJ/mol)	Δ*S* (J/mol)	Δ*G* (kJ/mol)
298	–16.30	–35.32	10.51
313			11.04
323			11.40
333			11.75

(Δ*S*°= –35.32 J/mol) showed decrease in randomness at the adsorbate–adsorbent interface during the adsorption of RhB onto biochar [7]. The Gibb's free energy was found to be positive at all the investigated temperatures. It increased from 10.51 to 11.75 kJ/mol with increasing temperature from 298 to 333 K which may be due to the intraction between adsorbent and adsorbate, with unbalanced competition imputed to heterogeneity of biochar surface and system received energy from external source at elevated temperatures [7,14]. In addition, the positive value of Gibb's free

energy represented that RhB adsorption onto biochars was non-spontaneous process.

4. Conclusions

In this work, RhB adsorption of from an aqueous solution onto UAE *Arecaceae* leaves biochar was investigated. FTIR spectroscopy demonstrated RhB adsorption onto the used adsorbent. The percentage removal of RhB was increased from 54% to 94%, and 8% to 94% with contact time and mass of UAE *Arecaceae* leaves biochar, respectively while decrease from 91% to 40% and 91% to 83% with initial concentration of RhB solution and temperature, respectively. Results of adsorption kinetic evaluation represented that RhB adsorption fitted to pseudo-second-order kinetic model. Adsorption of RhB onto UAE *Arecaceae* leaves biochar fitted well to Langmuir isotherm. The negative value of change in enthalpy ($\Delta H°$= –16.30 kJ/mol) showed that RhB adsorption onto UAE *Arecaceae* leaves biochar was exothermic process. Besides, the positive value of Gibb's free energy showed that RhB adsorption was non-spontaneous process. This study demonstrated that UAE *Arecaceae* leaves biochar could be employed as a extraordinary adsorbent for RhB adsorption from an aqueous solution.

Acknowledgements

The authors are highly thankful to University of Sharjah (UoS), Sharjah, United Arab Emirates for financial support.

References

[1] Á. Sánchez-Sánchez, F. Suárez-García, A. Martínez-Alonso, J.M.D. Tascón, Synthesis, characterization and dye removal capacities of N-doped mesoporous carbons, J. Colloid Interface Sci., 450 (2015) 91–100.
[2] M. Mohammadi, A.J. Hassani, A.R. Mohamed, G.D. Najafpour, Removal of Rhodamine B from aqueous solution using palm shell-based activated carbon: adsorption and kinetic studies, J. Chem. Eng. Data, 55 (2010) 5777–5785.
[3] A. Khaled, A.E. Nemr, A. El-Sikaily, O. Abdelwahab, Removal of Direct N Blue-106 from artificial textile dye effluent using activated carbon from orange peel: adsorption isotherm and kinetic studies, J. Hazard. Mater., 165 (2009) 100–110.
[4] Z. Wang, D. Shen, F. Shen, C. Wu, S. Gu, Kinetics, equilibrium and thermodynamics studies on biosorption of Rhodamine B from aqueous solution by earthworm manure derived biochar, Int. Biodeterior. Biodegrad., 120 (2017) 104–114.
[5] S. Rodríguez Couto, Dye removal by immobilised fungi, Biotechnol. Adv., 27 (2009) 227–235.
[6] M.I. Khan, A. Shanableh, N. Nasir, S. Shahida, Adsorptive removal of methyl orange from wastewaters by the commercial anion exchange membrane EPTAC, Desal. Water Treat., 234 (2021) 245–254.
[7] M.I. Khan, A. Shanableh, M.H. Lashari, S. Shahida, Application of the commercial anion exchange membrane for adsorptive removal of Eriochrome Black-T from aqueous solution, Desal. Water Treat., 252 (2022) 437–448.
[8] M.I. Khan, A. Shanableh, J. Fernandez, M.H. Lashari, S. Shahida, S. Manzoor, S. Zafar, A. ur Rehman, N. Elboughdiri, Synthesis of DMEA-grafted anion exchange membrane for adsorptive discharge of methyl orange from wastewaters, Membranes, 11 (2021) 166, doi: 10.3390/membranes11030166.
[9] A.A. Oyekanmi, A. Ahmad, K. Hossain, M. Rafatullah, Statistical optimization for adsorption of Rhodamine B dye from aqueous solutions, J. Mol. Liq., 281 (2019) 48–58.
[10] J. Mittal, A. Mariyam, F. Sakina, R.T. Baker, A.K. Sharma, A. Mittal, Batch and bulk adsorptive removal of anionic dye using metal/halide-free ordered mesoporous carbon as adsorbent, J. Cleaner Prod., 321 (2021) 129060, doi: 10.1016/j.jclepro.2021.129060.
[11] J.M. Asna Mariyam, F. Sakina, R.T. Baker, A.K. Sharma, Adsorption behaviour of Chrysoidine R dye on a metal/halide-free variant of ordered mesoporous carbon, Desal. Water Treat., 223 (2021) 425–433.
[12] S. Wang, Z. Zhu, A. Coomes, F. Haghseresht, G. Lu, The physical and surface chemical characteristics of activated carbons and the adsorption of methylene blue from wastewater, J. Colloid Interface Sci., 284 (2005) 440–446.
[13] M. Ahmed, R. Ram, Removal of basic dye from waste-water using silica as adsorbent, Environ. Pollut., 77 (1992) 79–86.
[14] M.I. Khan, A. Shanableh, Adsorption of Rhodamine B from an aqueous solution onto NaOH-treated rice husk, Desal. Water Treat., 252 (2022) 104–115.
[15] A. Mittal, J. Mittal, Chapter 11 – Hen Feather: A Remarkable Adsorbent for Dye Removal, S.K. Sharma, Ed., Green Chemistry for Dyes Removal from Wastewater: Research Trends and Applications, Wiley, United States of America, 2015, pp. 409–457.
[16] J. Mittal, Recent progress in the synthesis of layered double hydroxides and their application for the adsorptive removal of dyes: a review, J. Environ. Manage., 295 (2021) 113017, doi: 10.1016/j.jenvman.2021.113017.
[17] A. Çelekli, S.S. Birecikligil, F. Geyik, H. Bozkurt, Prediction of removal efficiency of Lanaset Red G on walnut husk using artificial neural network model, Bioresour. Technol., 103 (2012) 64–70.
[18] C. Arora, S. Soni, P.K. Bajpai, J. Mittal, A. Mariyam, Chapter 14 – Dye Removal From Waste Water Using Metal Organic Frameworks, P. Singh, C.M. Hussain, S. Rajkhowa, Eds., Management of Contaminants of Emerging Concern (CEC) in Environment, Elsevier, Amsterdam, Netherlands, 2021, pp. 375–394.
[19] I.H. Rais Ahmad, A. Mittal, Adsorption of Cr(VI) and Cd(II) on chitosan grafted polyaniline-OMMT nanocomposite: isotherms, kinetics and thermodynamics studies, Desal. Water Treat., 58 (2017) 144–153.
[20] A. Mariyam, J. Mittal, F. Sakina, R.T. Baker, A.K. Sharma, A. Mittal, Efficient batch and fixed-bed sequestration of a basic dye using a novel variant of ordered mesoporous carbon as adsorbent, Arabian J. Chem., 14 (2021) 103186, doi: 10.1016/j.arabjc.2021.103186.
[21] Y. Yang, D. Jin, G. Wang, D. Liu, X. Jia, Y. Zhao, Biosorption of Acid Blue 25 by unmodified and CPC-modified biomass of Penicillium YW01: kinetic study, equilibrium isotherm and FTIR analysis, Colloids Surf., B, 88 (2011) 521–526.
[22] R.A. Jyoti Mittal, A. Mittal, Kahwa tea (*Camellia sinensis*) carbon — a novel and green low-cost adsorbent for the sequestration of titan yellow dye from its aqueous solutions, Desal. Water Treat., 227 (2021) 404–411.
[23] S.S. Asha Patel, J. Mittal, A. Mittal, C. Arora, Sequestration of crystal violet from aqueous solution using ash of black turmeric rhizome, Desal. Water Treat,. 220 (2021) 342–352.
[24] R.-k. Xu, S.-c. Xiao, J.-h. Yuan, A.-z. Zhao, Adsorption of methyl violet from aqueous solutions by the biochars derived from crop residues, Bioresour. Technol., 102 (2011) 10293–10298.
[25] R.A. Jyoti Mittal, A. Mariyam, V.K. Gupta, A. Mittal, Expeditious and enhanced sequestration of heavy metal ions from aqueous environment by papaya peel carbon: a green and low cost adsorbent, Desal. Water Treat., 210 (2021) 365–376.
[26] P.K. Charu Arora, S. Soni, J. Mittal, A. Mittal, B. Singh, Efficient removal of malachite green dye from aqueous solution using *Curcuma caesia* based activated carbon, Desal. Water Treat., 195 (2020) 341–352.
[27] V. Kumar, P. Saharan, A.K. Sharma, A. Umar, I. Kaushal, A. Mittal, Y. Al-Hadeethi, B. Rashad, Silver doped manganese oxide-carbon nanotube nanocomposite for enhanced dye-sequestration: isotherm studies and RSM modelling approach, Ceram. Int., 46 (2020) 10309–10319.
[28] J.M. Asna Mariyam, F. Sakina, R.T. Baker, A.K. Sharma, Fixed-bed adsorption of the dye Chrysoidine R on ordered mesoporous carbon, Desal. Water Treat., 229 (2021) 395–402.

[29] S.A. Vinod Kumar Gupta, R. Ahmad, A. Mirza, J. Mittal, Sequestration of toxic congo red dye from aqueous solution using ecofriendly guar gum/activated carbon nanocomposite, Int. J. Biol. Macromol., (2020), doi: 10.1016/j.ijbiomac.2020.1005.1025.
[30] M.I. Khan, M.H. Lashari, M. Khraisheh, S. Shahida, S. Zafar, P. Prapamonthon, A. Rehman, S. Anjum, N. Akhtar, F. Hanif, Adsorption kinetic, equilibrium and thermodynamic studies of Eosin-B onto anion exchange membrane, Desal. Water Treat., 155 (2019) 84–93.
[31] M.A. Khan, M.I. Khan, S. Zafar, Removal of different anionic dyes from aqueous solution by anion exchange membrane, Membr. Water Treat., 8 (2017) 259–277.
[32] H. Zhu, R. Jiang, Y.-Q. Fu, J.-H. Jiang, L. Xiao, G.-M. Zeng, Preparation, characterization and dye adsorption properties of γ-Fe_2O_3/SiO_2/chitosan composite, Appl. Surf. Sci., 258 (2011) 1337–1344.
[33] M. Akgül, A. Karabakan, Promoted dye adsorption performance over desilicated natural zeolite, Microporous Mesoporous Mater., 145 (2011) 157–164.
[34] T. Farías, L.C. de Ménorval, J. Zajac, A. Rivera, Benzalkonium chloride and sulfamethoxazole adsorption onto natural clinoptilolite: effect of time, ionic strength, pH and temperature, J. Colloid Interface Sci., 363 (2011) 465–475.
[35] Y. Feng, F. Yang, Y. Wang, L. Ma, Y. Wu, P.G. Kerr, L. Yang, Basic dye adsorption onto an agro-based waste material–Sesame hull (*Sesamum indicum* L.), Bioresour. Technol., 102 (2011) 10280–10285.
[36] Y. Diquarternasi, Removal of basic blue 3 and reactive orange 16 by adsorption onto quartenized sugar cane bagasse, Malaysian J. Anal. Sci., 13 (2009) 185–193.
[37] M.I. Khan, S. Zafar,A.R. Buzdar, M.F. Azhar, W. Hassan, A. Aziz, Use of *Citrus sinensis* leaves as a bioadsorbent for removal of Congo red dye from aqueous solution, Fresenius Environ. Bull., 27 (2018) 4679–4688.
[38] M.I. Khan, S. Zafar, M.F. Azhar, A.R. Buzdar, W. Hassan, A. Aziz, M. Khraisheh, Leaves powder of *Syzgium cumini* as an adsorbent for removal of Congo red dye from aqueous solution, Fresenius Environ. Bull., 27 (2018) 3342–3350.
[39] M.I. Khan, T.M. Ansari, S. Zafar, A.R. Buzdar, M.A. Khan, F. Mumtaz, P. Prapamonthon, M. Akhtar, Acid green-25 removal from wastewater by anion exchange membrane: adsorption kinetic and thermodynamic studies, Membr. Water Treat., 9 (2018) 79–85.
[40] I. Ben Salem, M. El Gamal, M. Sharma, S. Hameedi, F.M. Howari, Utilization of the UAE date palm leaf biochar in carbon dioxide capture and sequestration processes, J. Environ. Manage., 299 (2021) 113644, doi: 10.1016/j.jenvman.2021.113644.
[41] H. Zhang, T. Lu, M. Wang, R. Jin, Y. Song, Y. Zhou, Z. Qi, W. Chen, Inhibitory role of citric acid in the adsorption of tetracycline onto biochars: effects of solution pH and Cu^{2+}, Colloids Surf., A, 595 (2020) 124731, doi: 10.1016/j.colsurfa.2020.124731.
[42] B. Sizirici, Y.H. Fseha, I. Yildiz, T. Delclos, A. Khaleel, The effect of pyrolysis temperature and feedstock on date palm waste derived biochar to remove single and multi-metals in aqueous solutions, Sustainable Environ. Res., 31 (2021) 9, doi: 10.1186/s42834-021-00083-x.
[43] C.H. Chia, B. Gong, S.D. Joseph, C.E. Marjo, P. Munroe, A.M. Rich, Imaging of mineral-enriched biochar by FTIR, Raman and SEM–EDX, Vib. Spectrosc., 62 (2012) 248–257.
[44] M. El Alouani, S. Alehyen, H. El Hadki, H. Saufi, A. Elhalil, O.K. Kabbaj, M. Taibi, Synergetic influence between adsorption and photodegradation of Rhodamine B using synthesized fly ash based inorganic polymer, Surf. Interfaces, 24 (2021) 101136, doi: 10.1016/j.surfin.2021.101136.
[45] J.B.G. Silva, E. Rigoti, S. Pergher, Rhodamine B adsorption in ordered mesoporous materials: a comparison efficiency on KIT-6 and CMK-8, Results Mater., 9 (2021) 100162, doi: 10.1016/j.rinma.2020.100162.
[46] S. Song, D. Wu, H. Zhao, Y. Cao, X. Wang, Y. Zhao, Fabrication of Co-FeOOH/g-C_3N_4 composite and its catalytic performance on heterogeneous photo-Fenton, Chin. J. Environ. Eng., 14 (2020) 3262–3269.
[47] F.A. Adekola, S.B. Ayodele, A.A. Inyinbor, Activated biochar prepared from plaintain peels: characterization and Rhodamine B adsorption data set, Chem. Data Collect., 19 (2019) 100170, doi: 10.1016/j.cdc.2018.11.012.
[48] J. Zhang, X. Hu, X. Yan, R. Feng, M. Zhou, J. Xue, Enhanced adsorption of Rhodamine B by magnetic nitrogen-doped porous carbon prepared from bimetallic ZIFs, Colloids Surf., A, 575 (2019) 10–17.
[49] S. Rahdar, A. Rahdar, M.N. Zafar, S.S. Shafqat, S. Ahmadi, Synthesis and characterization of MgO supported Fe–Co–Mn nanoparticles with exceptionally high adsorption capacity for Rhodamine B dye, J. Mater. Res. Technol., 8 (2019) 3800–3810.
[50] S.H. Alwan, H.A.H. Alshamsi, L.S. Jasim, Rhodamine B removal on A-rGO/cobalt oxide nanoparticles composite by adsorption from contaminated water, J. Mol. Struct., 1161 (2018) 356–365.
[51] A.A. Inyinbor, F.A. Adekola, G.A. Olatunji, Kinetics, isotherms and thermodynamic modeling of liquid phase adsorption of Rhodamine B dye onto Raphia hookerie fruit epicarp, Water Resour. Ind., 15 (2016) 14–27.
[52] M.I. Khan, S. Akhtar, S. Zafar, A. Shaheen, M.A. Khan, R. Luque, Removal of Congo red from aqueous solution by anion exchange membrane (EBTAC): adsorption kinetics and themodynamics, Materials, 8 (2015) 4147–4161.
[53] S. Zafar, M.I. Khan, M. Khraisheh, S. Shahida,T. Javed, M.L. Mirza, N. Khalid, Use of rice husk as an efective sorbent for the removal of cerium ions from aqueous solution: kinetic, equilibrium and thermodynamic studies, Desal. Water Treat., 150 (2019) 124–135.
[54] S. Zafar, M.I. Khan, H. Rehman, J. Fernandez-Garcia, S. Shahida, P. Prapamonthon, M. Khraisheh, A. Rehman, H.B. Ahmad, M.L. Mirza, N. Khalid, M.H. Lashari, Kinetic, equilibrium, and thermodynamic studies for adsorptive removal of cobalt ions by rice husk from aqueous solution, Desal. Water Treat., 204 (2020) 285–296.
[55] S. Zafar, M.I. Khan, M. Khraisheh, M.H. Lashari, S. Shahida, M.F. Azhar, P. Prapamonthon, M.L. Mirza, N. Khalid, Kinetic, equilibrium and thermodynamic studies for adsorption of nickel ions onto husk of *Oryza sativa*, Desal. Water Treat., 167 (2019) 277–290.

Supplementary information:

S1. Batch adsorption of Rhodamine B

Firstly, we prepared an aqueous solution of Rhodamine B (RhB) by dissolving a measured amount at room temperature. To investigate the effect of contact time on RhB adsorption onto UAE palm leaves biochars, the calculated quantity (0.30 g) was shaken into 20 mL of RhB aqueous solution with initial concentration of 20 mg/L at different time intervals such as 30, 60, 120, 180, 240, 300, 1,200 and 1,440 min at shaking speed of 200 rmp. The optimized mass of UAE palm leaves biochars was determined by shaking different quantities by varying mass from 0.05, 0.10, 0.15, 0.20, 0.25 and 0.30 g into 20 mL of RhB aqueous solution with initial concentration of 20 mg/L at shaking speed of 200 rmp at room temperature. The determined amount of UAE palm leaves biochar (0.30 g) was shaken at speed of 200 rmp into 20 mL of RhB aqueous solution with different initial concentration of RhB aqueous solution varying from 20, 25, 30, 35, 45, and 50 mg/L for 300 min at room temperature to determine adsorption isotherms. Similarly, the calculated amount of UAE palm leaves biochar (0.30 g) was shaken at 298, 313, 323 and 333 K for 300 min at speed 200 rmp into 20 mL of RhB aqueous solution with initial concentration of 20 mg/L to study adsorption thermodynamics. The RhB concentration was measured by utilizing UV-Vis Spectrophotometer (UV-2550, Shimadzu, Kyoto, Japan) by calculating the absorbance of the supernatant at wavelength (λ_{max} = 556 nm for RhB). The RhB concentration of was measured by employing calibration curve. The removal of RhB was measured by utilizing the relationship Eq. (S1):

$$\text{Removal} = \frac{C_o - C_t}{C_o} \times 100 \tag{S1}$$

where C_o and C_t are concentrations of RhB at initial state and at time t, respectively. Similarly, V is volume of dye aqueous solution and W is the mass of UAE *Arecaceae* leaves biochar.

S2. Adsorption isotherms

S2.1. Langmuir isotherm

It is based on the maximum adsorption corresponding to the saturated monolayer of liquid molecules on the solid surface. It is expressed as [S1].

$$\frac{C_e}{q_e} = \frac{1}{K_L Q_m} + \frac{C_e}{Q_m} \tag{S2}$$

where C_e is supernatant concentration at equilibrium state of the system (mg/L), Q_m is Langmuir monolayers adsorption capacity, K_L is Langmuir constant (L/mg)(mg/g), and q_e is the amount of dye adsorbed at equilibrium state of system (mg/g). The Langmuir isotherm essential characteristics can be shown in term of dimensionless constant separation factor R_L that is expressed as [S2].

$$R_L = \frac{1}{1 + K_L C_o} \tag{S3}$$

The value of R_L showed the shape of the isotherm to be either unfavorable (R_L > 1), linear (R_L = 1), favorable (0 < R_L > 0), or irreversible (R_L = 0) [S3].

S2.2. Freundlich isotherm

It is utilized to explain heterogeneous system. It is shown as [S4]:

$$\log q_e = \log K_f + \frac{1}{n} \log C_e \tag{S4}$$

where K_f and n_F are Freundlich constant.

S2.3. Temkin isotherm

It is given as [S5]:

$$q_e = B_T \ln A_T + B_T \ln C_e \tag{S5}$$

where B_T = RT/b_T, R is gas constant (8.31 J/mol·K) and T is absolute temperature (K). The constant b_T is related to the heat of adsorption and A_T is equilibrium binding constant coinciding to the maximum binding energy.

S2.4. Dubinin–Radushkevich (D-R) isotherm

It is represented as [S5]:

$$\ln q_e = \ln q_m - \beta \varepsilon^2 \tag{S6}$$

where β (mol²/kJ) is constant related to the adsorption energy and ε is the Polanyi potential can be measured by employing the Eq. (S7).

$$\varepsilon = RT \ln\left(1 + \frac{1}{C_e}\right) \tag{S7}$$

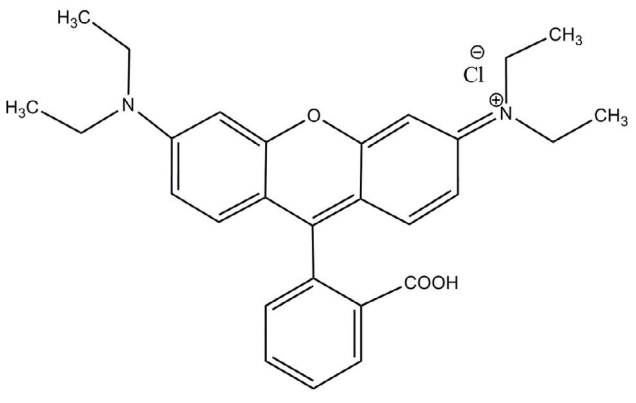

Fig. S1. Chemical structure of Rhodamine B dye.

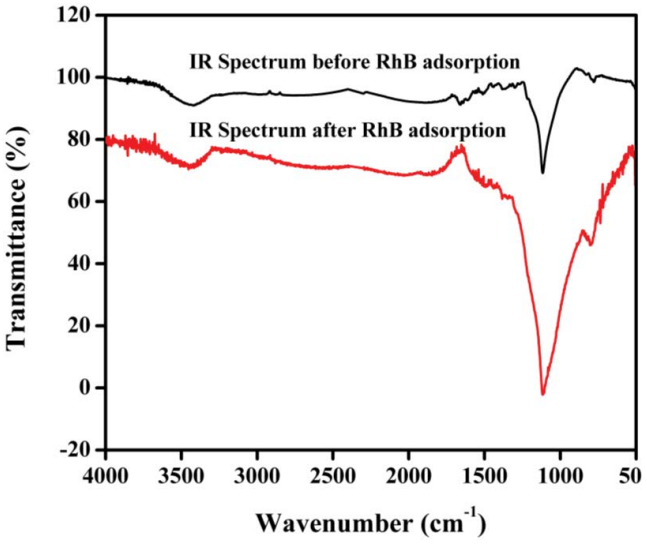

Fig. S2. FTIR spectrum of biochars before and after RhB adsorption.

where R is gas constant (8.31 kJ/mol) and T is absolute temperature (K). The mean free energy E (kJ/mol) can be determined by the relationship Eq. (S8).

$$E = \frac{1}{\sqrt{2\beta}} \tag{S8}$$

S3. Adsorption kinetics

S3.1. Pseudo-first-order model

It is shown as [S6–S9]:

$$\log\left(q_e - q_t\right) = \log q_e - \frac{k_1 t}{2.303} \tag{S9}$$

where k_1 (/min), q_e and q_t represent rate constant of pseudo-first-order model, concentration of RhB adsorbed at equilibrium and time t, respectively.

S3.2. Pseudo-second-order model

Its linear form is represented as [S9,S10]:

$$\frac{t}{q_t} = \frac{1}{k_2 q_e^2} + \frac{t}{q_e} \tag{S10}$$

where k_2 (g/mg·min) is the rate constant of pseudo-second-order model.

S3.3. Elovich model

It is given as [S11,S12]:

$$q_t = \frac{1}{\beta}\ln\left(\alpha\beta\right) + \frac{1}{\beta}\ln t \tag{S11}$$

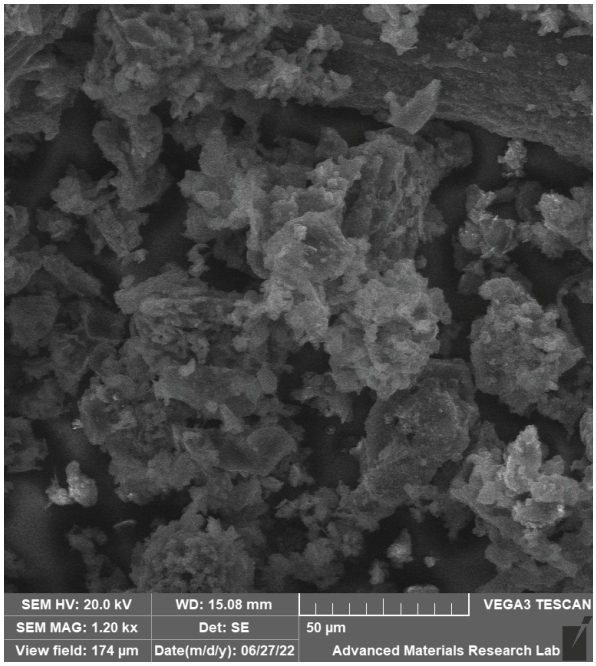

Fig. S3. SEM image presenting the morphology of palm leaves biochar.

where α (mg/g·min) and β (g/mg) are constant. The α show the initial adsorption rate and β the extent of surface coverage and activation energy for chemisorption.

S3.4. Liquid-film diffusion model

It is shown expressed as [S13]:

$$\mathrm{Ln}\left(1 - F\right) = -K_{\mathrm{fa}} t \tag{S12}$$

where K_{fd} is liquid-film diffusion rate constant and $F = q_t/q$.

S3.5. Modified Freundlich equation

It was originally developed by Kuo and Lotse [S10,S14]:

$$q_t = kC_o t^{1/m} \tag{S13}$$

where k, C_o, t and m are adsorption rate constant (L/g·min), initial concentration of dye (mg/L), contact time (min) and the Kuo–Lotse constant, respectively. Its linear form is given as:

$$\ln q_t = \ln\left(kC_o\right) + \frac{1}{m}\ln t \tag{S14}$$

S3.6. Bangham equation

It is represented as [S9,S12]:

$$\log\log\left(\frac{C_o}{C_o - q_t m}\right) = \log\left(\frac{k_o m}{2.303V}\right) + \alpha\log t \tag{S15}$$

where m is mass of the adsorbent used (g/L), V is volume of adsorbate (mL), α (<1) and k_o (mL/(g/L) are constants.

S4. Adsorption thermodynamics

The values of change in Gibb's free energy (ΔG°), enthalpy (ΔH°) and entropy (ΔS°) were measured by using the Eqs. (S16)–(S18):

$$\ln K_c = \frac{\Delta S^\circ}{R} - \frac{\Delta H^\circ}{RT} \tag{S16}$$

$$K_c = \frac{C_a}{C_e} \tag{S17}$$

$$\Delta G^\circ = \Delta H^\circ - T\Delta S^\circ \tag{S18}$$

where K_c, ΔG°, ΔH° and ΔS° are equilibrium constant, change in Gibb's free energy (kJ/mol), enthalpy (kJ/mol) and entropy (J/mol·K), respectively.

References

[S1] I. Langmuir, The constitution and fundamental properties of solids and liquids, J. Franklin Inst. 183 (1917) 102–105.
[S2] T.W. Weber, R.K. Chakravorti, Pore and solid diffusion models for fixed-bed adsorbers, AIChE J. 20 (1974) 228–238.
[S3] G. McKay, Adsorption of dyestuffs from aqueous solutions with activated carbon I: Equilibrium and batch contact-time studies, J. Chem. Technol. Biotechnol. 32 (1982) 759–772.
[S4] H. Freundlich, Uber die adsorption in lasugen (Leipzig), Z. Phys. Chem. A, 57 (1906) 385–470.
[S5] M.I. Khan, S. Zafar, M.A. Khan, F. Mumtaz, P. Prapamonthon, .R. Buzdar, Bougainvillea glabra leaves for adsorption of congo red from wastewater, Fresenius Environ. Bull. 27 (2018) 1456–1465.
[S6] S. Zafar, M.I. Khan, M. Khraisheh, S. Shahida,Tariq Javed, M.L. Mirza, N. Khalid, Use of rice husk as an efective sorbent for the removal of cerium ions from aqueous solution: kinetic, equilibrium and thermodynamic studies, Desal. Water Treat. 150 (2019) 124–135.
[S7] M.I. Khan, S. Zafar, A.R. Buzdar, M.F. Azhar, W. Hassan, A. Aziz, Use of citrus sinensis leaves as a bioadsorbent for removal of congo red dye from aqueous solution, Fresenius Environ. Bull. 27 (2018) 4679–4688.
[S8] M.I. Khan, S. Zafar, M.F. Azhar, A.R. Buzdar, W. Hassan, A. Aziz, M. Khraisheh, Leaves powder of syzgium cumini as an adsorbent for removal of congo red dye from aqueous solution, Fresenius Environ. Bull. 27 (2018) 3342–3350.
[S9] M.I. Khan, A. Shanableh, J. Fernandez, M.H. Lashari, S. Shahida, S. Manzoor, S. Zafar, A. ur Rehman, N. Elboughdiri, Synthesis of DMEA-Grafted Anion Exchange Membrane for Adsorptive Discharge of Methyl Orange from Wastewaters, Membranes, 11 (2021) 166.
[S10] M.I. Khan, M.H. Lashari, M. Khraisheh, S. Shahida, S. Zafar, P. Prapamonthon, A. Rehman, S. Anjum, N. Akhtar, F. Hanif, Adsorption kinetic, equilibrium and thermodynamic studies of Eosin-B onto anion exchange membrane, Desal. Water Treat. 155 (2019) 84–93.
[S11] M.A. Khan, M.I. Khan, S. Zafar, Removal of different anionic dyes from aqueous solution by anion exchange membrane, Membr. Water Treat. 8(2017) 259–277.
[S12] M.I. Khan, S. Akhtar, S. Zafar, A. Shaheen, M.A. Khan, R. Luque, Removal of Congo Red from Aqueous Solution by Anion Exchange Membrane (EBTAC): Adsorption Kinetics and Themodynamics, Materials, 8 (2015) 4147–4161.
[S13] L. Liu, Y. Lin, Y. Liu, H. Zhu, Q. He, Removal of Methylene Blue from Aqueous Solutions by Sewage Sludge Based Granular Activated Carbon: Adsorption Equilibrium, Kinetics, and Thermodynamics, J. Chem. Eng. Data, 58 (2013) 2248–2253.
[S14] M.I. Khan, J. Su, L. Guo, Development of triethanolamine functionalized-anion exchange membrane for adsorptive removal of methyl orange from aqueous solution, Desal. Water Treat. 209 (2021) 342–352.